PET/MRI early after myocardial infarction: evaluation of viability with late gadolinium enhancement transmurality vs. ^{18}F-FDG uptake

Christoph Rischpler[1,3][†]*, Nicolas Langwieser[2][†], Michael Souvatzoglou[1], Anja Batrice[2], Sandra van Marwick[1], Julian Snajberk[2], Tareq Ibrahim[2], Karl-Ludwig Laugwitz[2,3], Stephan G. Nekolla[1,3][‡], and Markus Schwaiger[1,3][‡]

[1]Nuklearmedizinische Klinik und Poliklinik, Klinikum rechts der Isar, Technische Universität München, Ismaninger Strasse 22, 81675 Munich, Germany; [2]Medizinische Klinik und Poliklinik I, Klinikum rechts der Isar, Technische Universität München, Munich, Germany; and [3]DZKH (Deutsches Zentrum für Herz-Kreislauf-Forschung e.V.), Partner Site Munich Heart Alliance, Munich, Germany

Aims   F-18 fluorodeoxyglucose (FDG) myocardial PET imaging is since more than two decades considered to delineate glucose utilization in dysfunctional but viable cardiomyocytes. Late gadolinium enhancement (LGE) MRI was introduced more than a decade ago and identifies increased extravascular space in areas of infarction and scar. Although the physiological foundation differs, both approaches are valuable in the prediction of functional outcome of the left ventricle, but synergistic effects are yet unknown. We aimed to compare the improvement of LV function after 6 months based on the regional FDG uptake and the transmurality of scar by LGE in patients early after acute myocardial infarction (AMI).

Methods and results   Twenty-eight patients with primary AMI underwent simultaneous PET/MRI for assessment of regional FDG uptake and degree of LGE transmurality 5−7 days after PCI. Follow-up by MRI was performed in 20 patients 6 months later. Myocardium was defined 'PET viable' based on the established threshold of ≥50% FDG uptake compared with remote myocardium or as 'MRI viable' when LGE transmurality of ≤50% was present. Regional wall motion was measured by MRI. Ninety-five dysfunctional segments were further analysed regarding regional wall motion recovery. There was a substantial intermethod agreement for segmental LGE transmurality and reduction of FDG uptake ($\kappa = 0.65$). 'PET viable' and 'MRI viable' segments showed a lower wall motion abnormality score (PET: initial: 1.4 ± 0.6 vs. 1.9 ± 0.8, $P < 0.008$; follow-up: 0.5 ± 0.7 vs. 1.5 ± 1.0, $P < 0.0001$; MRI: initial: 1.5 ± 0.6 vs. 2.0 ± 0.8, $P < 0.002$; follow-up: 0.7 ± 0.8 vs. 1.6 ± 1.0, $P < 0.0001$) and a better regional wall motion improvement (PET: -0.9 ± 0.7 vs. -0.4 ± 0.7, $P < 0.0007$; MRI: -0.8 ± 0.7 vs. -0.4 ± 0.7, $P < 0.009$) compared with 'PET non-viable' or 'MRI non-viable' segments, respectively. Eighteen per cent of the dysfunctional segments showed discrepant findings ('PET non-viable' but 'MRI viable'). At follow-up, the regional wall motion of these segments was inferior compared with 'PET viable/MRI viable' segments (1.1 ± 0.8 vs. 0.5 ± 0.7, $P < 0.01$), had an inferior functional recovery (-0.5 ± 0.6 vs. -0.9 ± 0.7, $P < 0.03$), but showed no difference compared with concordant 'PET non-viable/MRI non-viable' segments.

Conclusion   The simultaneous assessment of LGE and FDG uptake using a hybrid PET/MRI system is feasible. The established PET and MRI 'viability' parameter prior to revascularization therapy also predicts accurately the regional outcome of wall motion after AMI. In a small proportion of segments with discrepant FDG PET and LGE MRI findings, FDG uptake was a better predictor for functional recovery.

Keywords   PET/MRI • Viability • FDG • Late gadolinium enhancement • Myocardial infarction • Wall motion recovery

* Corresponding author. Tel: +49 163 7227772; Fax: +49 89 41404841, E-mail: c.rischpler@tum.de; rischpler@gmail.com

[†] Both first authors contributed equally to this article.

[‡] Both senior authors contributed equally to this article.

Introduction

Early after acute myocardial infarction (AMI), the discrimination between reversible and irreversible myocardial dysfunction is of high clinical interest. In patients suffering from chronic ischaemic heart disease, 'viability' imaging by PET and late gadolinium enhancement (LGE) imaging using MRI are established techniques to predict whether patients will have an improved left ventricular (LV) function and improved survival after revascularization.[1,2] In the subacute phase after AMI, however, studies investigating these techniques are scarce.

The gold standard to distinguish patients with reversible from those with irreversible myocardial dysfunction is F-18 fluorodeoxyglucose (FDG) PET imaging.[3] The underlying principle is that ischaemically injured myocardium demonstrates a shift in myocardial metabolism from the oxidation of free fatty acids towards glucose utilization.[4] Hibernating myocardium, a state caused by chronic hypoperfusion or repetitive stunning, is dysfunctional and metabolizes primarily glucose. This up-regulation of glucose utilization in myocardium exposed to ischaemia is associated with poor outcome[5] and the amount of hypoperfused but reversible injured myocardium—a state called mismatch—is of prognostic significance.[1,6] Myocardium with reduced blood flow but preserved or up-regulated FDG uptake has the potential to recover after revascularization.[7]

An alternative imaging method is the late LGE technique by cardiac MRI. MR imaging is performed 5–20 min after the administration of gadolinium-DTPA using inversion-recovery prepared T1-weighted gradient-echo pulse sequences to suppress the signal from remote myocardium and allows the identification of scarred myocardium as signal-enhanced areas.[8,9] Due to the high resolution of MRI, transmural infarction can be distinguished from non-transmural LGE. Furthermore, even small areas of subendocardial infarction can be detected which is also known to be of prognostic relevance.[10]

The specificity for the prediction of functional recovery after revascularization is—according to a recent meta-analysis—comparable for FDG PET and LGE MR imaging (~63%), while PET showed higher sensitivity (92 vs. 84%).[3] However, there are fundamental differences for the assessment of reversibly damaged myocardium between the two imaging modalities: while LGE primarily depicts increased extracellular space associated with scar tissue, the FDG uptake represents a true metabolic signal of viable cells.

The ongoing emergence of combined PET/MRI scanners offers the unique opportunity to directly compare these different but potentially complementary modalities in a simultaneous imaging session at identical conditions with best achievable co-registration. So far, studies investigating FDG PET imaging shortly after revascularization are scarce, especially with follow-up imaging for the determination of LV function changes.[11] In this study, patients were imaged in the subacute phase after AMI using both FDG PET and MRI for LGE, LV function, and wall motion assessment. We aimed to compare the improvement of LV function based on the regional FDG uptake and the transmurality of scar by LGE in patients early after AMI.

Methods

Patient population

Patients suffering from primary AMI between 1 November 2011 and 1 September 2012 who were treated by primary angioplasty of the infarct-related artery immediately after hospital admission and who had no contraindications for PET/MRI (pregnancy, haemodynamic instability, creatinine clearance <50 mL/min, allergy to contrast agent, claustrophobia, presence of pacemakers, ICDs, or any other ferromagnetic material in the body) were included in this study. AMI was defined by chest pain lasting at least 20 min (onset of symptoms <72 h before PCI) associated with electrocardiographic (ECG) changes (ST-segment elevation, new-onset left bundle branch block) and/or elevated cardiac enzyme levels. The simultaneous FDG PET/MRI scan was performed 5–7 days after PCI in 28 patients. Follow-up imaging by MRI only was scheduled to take place ~6 months after PCI. In seven patients, the scheduled follow-up imaging could not be obtained due to MRI-incompatible pacemaker/ICD implantation ($n = 3$) or due to loss to follow-up ($n = 4$). Furthermore, one patient had to be removed from the final analysis because of poor image quality of the initial scan. Consequently, the final study population consisted of 20 patients who underwent both initial and follow-up imaging and whose scans showed good image quality.

Simultaneous PET/MR imaging was performed 5.6 ± 1.4 days after hospital admission (baseline), and follow-up imaging by MRI only was performed after 194 ± 22 days. In the final study group, there were 11 (55%) men and 9 (45%) women with a mean age of 59.4 ± 15.0 years and a mean body mass index of 26.7 ± 4.8 (range: 18.8–35.1) kg/m². Regarding risk factors as defined by published criteria,[12–15] there were 11 (55%) patients with a history of smoking, 14 (70%) subjects suffering from hypertension, 11 (55%) patients with dyslipidaemia, 2 (10%) subjects with diabetes mellitus, and 3 (15%) patients had a positive family history of premature coronary artery disease. In 15 patients (75%), an ST-segment elevation myocardial infarction (STEMI) was diagnosed, whereas 5 patients (25%) had a non-ST-segment elevation myocardial infarction (NSTEMI). The infarct location was anterior in 13 patients (65%), inferior in 4 patients (20%), and lateral in 3 patients (15%). PCI was performed on average 11.2 (range: 8.2–13.6) h after onset of symptoms. Peak level of creatine kinase prior to PCI was 508 (range: 302–799) U/L. General patient characteristics and further details on the infarct properties are given in *Table 1*.

The study was approved by the local ethics committee and was performed in agreement with the ethical standards according to the Declaration of Helsinki. For all patients written informed consent was obtained prior to imaging.

Imaging protocol

Imaging was performed in all patients using a hybrid PET/MRI system (Biograph mMR, Siemens Medical Solutions, Erlangen, Germany) which allows the simultaneous acquisition of PET and MRI data in a single session. The MRI component of this scanner consists of a 3-T MRI scanner, while the PET component is built of LSO crystals equipped with avalanche photodiodes.[16] The performance of the scanner has been previously evaluated in different studies.[17–21]

PET imaging

To standardize the metabolic environment in all patients, the hyperinsulinaemic-euglycaemic clamp technique was applied as previously described.[22,23] 65 ± 18 min after the intravenous injection of 300 ± 62 MBq of FDG, a list-mode PET scan in 3D mode was started. The acquisition was performed applying ECG gating. Correction of the emission data was performed for dead time, randoms, scatter, and attenuation. The acquired images were reconstructed using a 3D attenuation-weighted ordered subsets expectation maximization iterative reconstruction algorithm (AW-OSEM 3D) with three iterations and 21 subsets, Gaussian smoothing at 4 mm full width at half maximum, a matrix size of 344 × 344, and a zoom of 1.[18] Attenuation correction of the acquired PET data was accomplished using 2-point

Table I General patient characteristics and further details on the infarct properties

Variable	(n = 20)
Age, years	59.4 ± 15.0 [22−79]
Gender	
Men	11 (55%)
Women	9 (45%)
Body mass index (kg/m^2)	26.7 ± 4.8 [18.8−35.1]
Cardiovascular risk factors	
Smoking	11 (55%)
Hypertension	14 (70%)
Dyslipidaemia	11 (55%)
Diabetes mellitus	2 (10%)
Family history	3 (15%)
Infarct location	
Anterior	13 (65%)
Inferior	4 (20%)
Lateral	3 (15%)
ECG	
STEMI	15 (75%)
NSTEMI	5 (25%)
Cardiac markers (before PCI)	
CK, U/L	508 ± 475 [302−799]
CK-MB, U/L	57 ± 59 [27−96]
Troponin T, ng/mL	0.52 ± 0.54 [0.2−0.9]
Time to balloon, h	11.2 ± 9.1 [8.2−13.6]
TIMI flow grade before PCI	
0	11 (55%)
1	2 (10%)
2	5 (25%)
3	2 (10%)
TIMI flow grade post-PCI	
0	1 (5%)
1	0
2	1 (5%)
3	18 (90%)
EF before angioplasty, %	43 ± 6 [40−48]

Patients in this group underwent initial PET/MR imaging 5.6 ± 1.4 days after hospital admission due to AMI. Follow-up imaging by MRI only was performed after 193.8 ± 22.8 days.

Dixon MRI sequences as previously described.[24] As parts of the body—especially the arms—are often truncated in the attenuation map by the MRI due to the relatively small field of view that is also smaller than the field of view of the PET component, the missing part of the attenuation map was recovered from PET emission data using the so-called maximum likelihood reconstruction of attenuation and activity (MLAA) technique as previously described.[25]

MR imaging

For the assessment of LGE, phase-sensitive, inversion-recovery prepared T1-weighted gradient-echo pulse sequences (PSIRS)[26] were acquired 10 min after the intravenous administration of 0.2 mmol Gadopentetat-Dimeglumin (Magnograf®; Marotrast GmbH, Jena, Germany) per kilogram body weight. For left ventricular wall motion analyses, steady-state free precession cine sequences were acquired. ECG triggering was applied for the acquisition of these sequences, and all images—including long-axis (two-chamber view and four-chamber view) and short-axis views of the entire left ventricle—were obtained during breath hold. For the entire scan, phased-array body surface coils were used.

Image analyses

For the image analyses, the 17-segment model according to the American Heart Association (AHA)[27] was applied to the short- and long-axis myocardial tomograms of each acquired data set, namely the LGE images, the FDG PET images, and the cine sequences and subsequently processed as follows.

MRI

Transmurality of LGE and wall motion were assessed as described previously.[2,28] Briefly, based on prior studies, transmurality of LGE was determined in each segment (according to the AHA 17-segment model), and if the proportion was ≤50%, the underlying myocardium was defined as 'MRI viable' or as 'MRI non-viable' if LGE was transmural (proportion >50%), respectively.[2,29,30] To analyse identical segments in LGE and FDG PET images, regions of interest (ROIs) according to the AHA 17 segment model were defined on LGE images and then subsequently applied to the corresponding PET images (Figure 1A). Also, the degree of wall motion abnormality in each of the 17 myocardial segments was evaluated based on the extent of wall thickening using a 5-point scale as previously described: 0 = normal wall motion, 1 = mild to moderate hypokinesia, 2 = severe hypokinesia, 3 = akinesia, and 4 = dyskinesia.[2] A functional improvement of wall motion was defined as a decrease of the wall motion score of at least 1 point score. Two experienced observers performed all analyses. In case of disagreement, a third observer reviewed the study and the resulting majority judgment was binding regarding the segmental grading.

To calculate LV function parameters (such as ESV, EDV, and EF), the contours of the whole left ventricle were outlined on short-axis cine images using the MunichHeart/MR software. Furthermore, the extent of LGE in the whole LV myocardium was determined by manual delineation on short-axis images using the MunichHeart/MR software and expressed as percentage of the left ventricle.[31]

PET

For the assessment of regional FDG uptake, summed FDG PET images were analysed using the MunichHeart (/NM, /Anima) software, a well-established custom application that has been previously validated for quantitative PET analyses.[32,33] To determine the spatial distribution of FDG in the LV myocardium, volumetric sampling was performed, and a static polar map of 460 segments was created. In a completely automated process, the software then determined the region with the maximal uptake of FDG within the left ventricle, which was defined as the reference ROI and set as 100% (Figure 1B). If the FDG uptake in the respective, analysed segment was at least 50% of the previously determined threshold, the respective segment was defined as 'FDG viable' based on prior studies.[34] Accordingly, in case of an FDG uptake below this threshold, the respective segment was deemed 'FDG non-viable'.

Statistics

All results are shown as mean ± standard deviation. Obtained P values <0.05 were considered to indicate statistical significance. To compare continuous variables, the two-tailed unpaired Student's t-test was applied. The association between continuous variables was investigated using the Pearson correlation coefficient. Categorical intermethod agreement between regional LGE transmurality in MRI and FDG uptake in PET
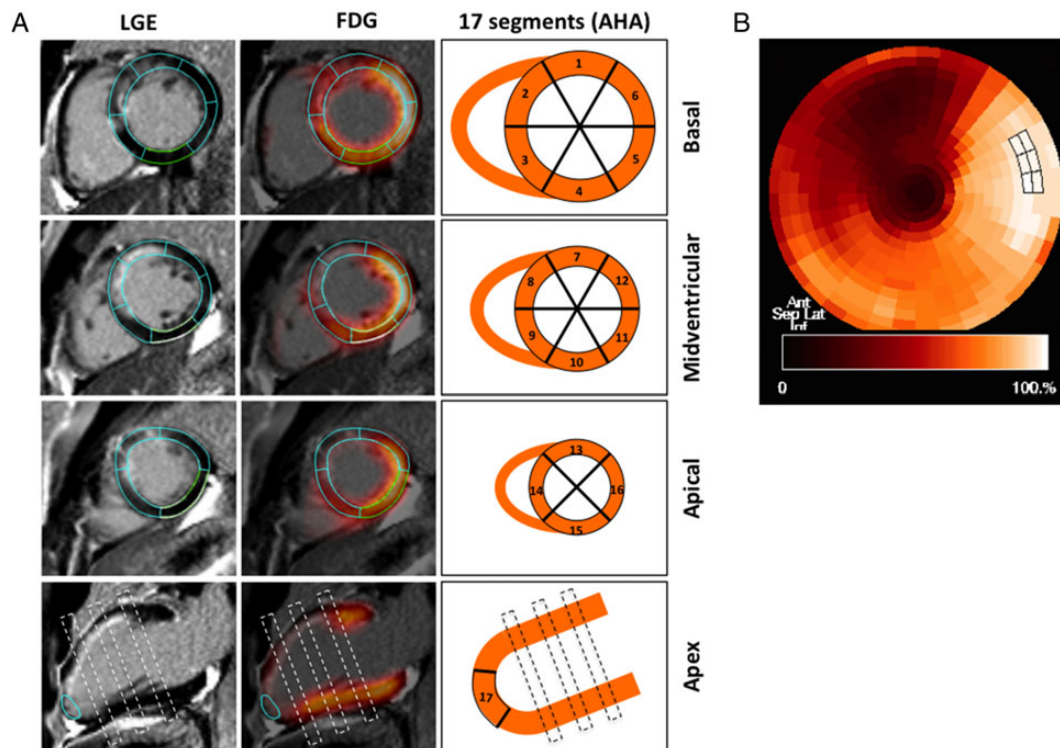
Figure 1 Analysis of segmental FDG uptake and LGE transmurality. Segmental FDG uptake and LGE transmurality were analysed according to the AHA 17-segment model (*A*, third column). ROIs were first drawn on a basal, a midventricular, and an apical slice and in the apex in LGE images (*A*, first column: light blue ROIs in LGE images) and then automatically transferred to identical slices of ideally fused FDG/LGE images (*A*, second column). LGE in these 17 segments was visually judged as transmural ('MRI non-viable') or non-transmural ('MRI viable') if the LGE transmurality proportion was >50 or ≤50%, respectively. If the FDG uptake in the assessed segment was ≥50% or <50%, respectively, compared with an automatically determined reference ROI encompassing the maximal uptake in the left ventricle, the segment was graded as 'PET viable' or 'PET non-viable' (*B*, the highlighted six sectors in the static polar map represent the reference ROI set as 100%).

was assessed by the Cohen κ (κ < 0, poor agreement; κ = 0–0.20, slight agreement; κ = 0.40–0.60, moderate agreement; κ = 0.60–0.80, substantial agreement; κ = 0.80–1.00, very good agreement).

For statistical analyses, MedCalc (version 12.7.2.0; MedCalc Software) for Windows (Microsoft) was used.

Results

Global left ventricular parameters

LV (ESV, EDV, and SV) volumes of the entire study group did not change significantly between initial and the follow-up imaging. The EF early after AMI was $50 \pm 10\%$ and did not change over time [$52 \pm 11\%$ at follow-up; $P > 0.05$ (NS)].

The LGE extent of the left ventricle was $22 \pm 9\%$ early after myocardial infarction and decreased to $19 \pm 8\%$ at follow-up ($P < 0.01$).

Regional analyses

Of the 20 patients included in the final analyses, a total of 340 myocardial segments (according to the AHA 17-segment model) were semi-quantitatively evaluated regarding wall motion abnormalities at baseline as well as at follow-up imaging ~6 months later. Ninety-five

segments (95/340, 28%) showed wall motion abnormalities at baseline, and the mean wall motion abnormality score of these segments was 1.7 ± 0.8. At follow-up, the mean wall motion abnormality score of these 95 segments decreased significantly to 1.1 ± 1.0 ($P < 0.0001$).

Regional assessment of LGE transmurality and FDG uptake at baseline

Analysis of LGE transmurality and FDG uptake resulted in the following distribution (*Table 2*):

- PET viable and MRI viable: 34%
- PET non-viable and MRI non-viable: 48%
- PET viable, but MRI non-viable: 0%
- PET non-viable, but MRI viable: 18%.

This results in an overall agreement between LGE transmurality and FDG uptake of 82% (78 of the 95 dysfunctional segments) with a substantial intermethod agreement (κ = 0.65). Examples illustrating the different observed LGE transmurality/FDG uptake patterns are displayed in *Figure 2*.

Table 2 Distribution of the dysfunctional segments at baseline and their functional recovery at follow-up based on segmental FDG uptake and/or LGE transmurality

PET/MRI	Number of dysfunctional segments at baseline ($n = 95$)		Wall motion recovery at follow-up	
	(n)	(%)	(n)	(%)
Separate analysis				
MRI viable[a]	49	52	32	65
MRI non-viable[b]	46	48	15	33
PET viable[c]	32	34	25	78
PET non-viable[d]	63	66	22	35
Integrated analysis				
PET viable[c]/MRI viable[a]	32	34	25	78
PET non-viable[d]/MRI non-viable[b]	46	48	15	33
PET viable[c]/MRI non-viable[b]	0	0	–	–
PET non-viable[d]/MRI viable[a]	17	18	7	41

Ninety-five myocardial segments of the 340 segments (according to the AHA 17-segment model), which were evaluated at baseline, showed wall motion abnormalities. These segments were investigated regarding LGE transmurality and regional FDG uptake. At follow-up, the presence of functional recovery of these segments was assessed.
[a]MRI viable: LGE $\leq$ 50%.
[b]MRI non-viable: LGE $>$ 50%.
[c]PET viable: FDG $\geq$ 50%.
[d]PET non-viable: FDG $<$ 50%.

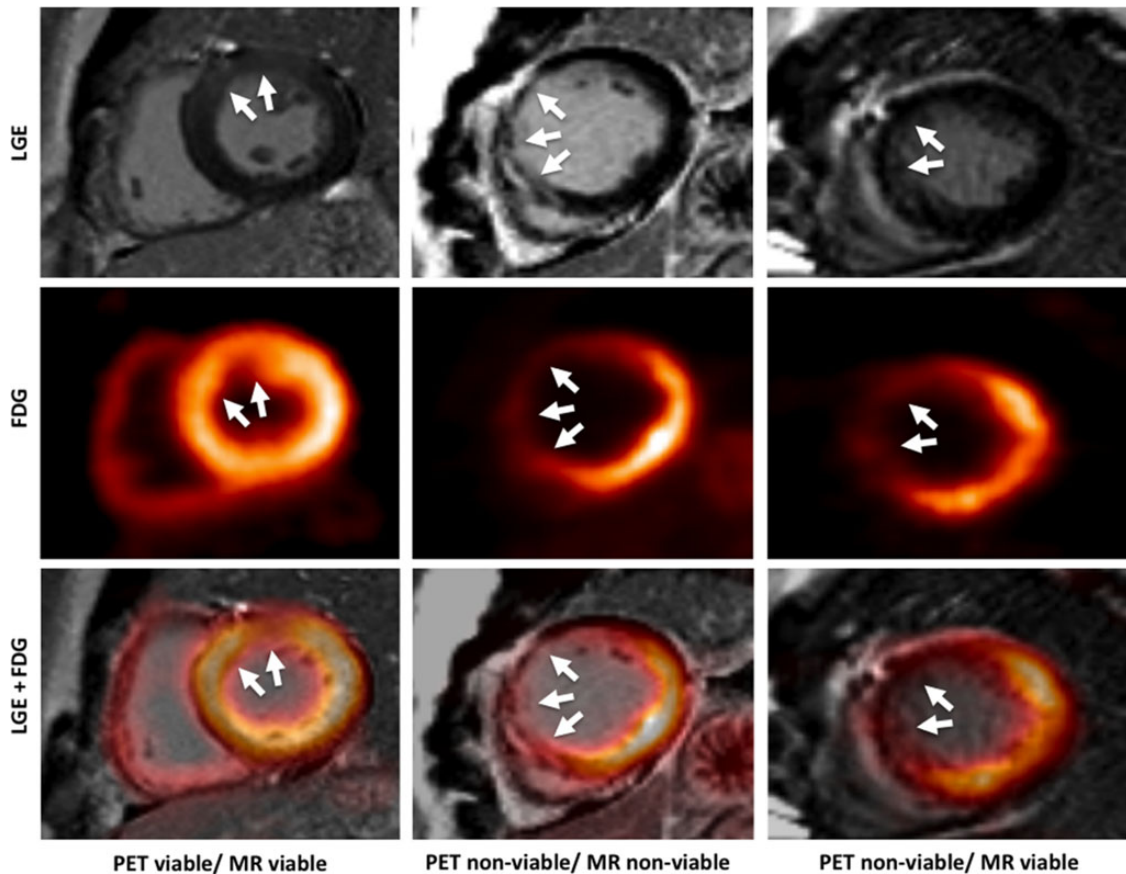PET viable/ MR viable   PET non-viable/ MR non-viable   PET non-viable/ MR viable

Figure 2 Images illustrating different combinations of FDG uptake and LGE transmurality. First column: FDG $\geq$ 50%/LGE non-transmural ('PET viable/MRI viable'); second column: FDG $<$ 50%/LGE transmural ('PET non-viable/MRI non-viable'); third column: FDG $<$ 50%/LGE non-transmural ('PET non-viable/MRI viable'). White arrows indicate the respective area of ischaemically affected myocardium.

Regional wall motion abnormality

Initial imaging

Early after revascularization, the wall motion abnormality score of MRI non-viable segments was significantly higher than that of MRI viable segments (2.0 ± 0.8 vs. 1.5 ± 0.6, $P < 0.002$) (*Figure 3A* left). Also, the wall motion abnormality score was significantly higher in PET non-viable segments as opposed to PET viable segments (1.9 ± 0.8 vs. 1.4 ± 0.6, $P < 0.008$) (*Figure 3B* left).

When comparing the wall motion abnormality scores of the different groups of the integrated PET/MRI analyses, the following results were observed: as expected, the wall motion abnormality score of the 'PET viable/MRI viable' group was significantly lower compared with the 'PET non-viable/MRI non-viable' group (1.4 ± 0.6 vs. 2.0 ± 0.8, $P < 0.002$). Interestingly, no difference in the wall motion abnormality score was found between the 'PET non-viable/MRI non-viable' group and the 'PET non-viable/MRI viable' group (2.0 ± 0.8 vs. 1.6 ± 0.7, $P = $ NS). Also, no difference was present between the 'PET viable/MRI viable' and the 'PET non-viable/MRI viable' group (1.4 ± 0.6 vs. 1.6 ± 0.7, $P = $ NS) (*Figure 3C* left).

Follow-up imaging

At follow-up, the wall motion of 'MRI non-viable' segments was still significantly impaired compared with 'MRI viable' segments (1.6 ± 1.0 vs. 0.7 ± 0.8, $P < 0.0001$) (*Figure 3A* right), and the wall motion abnormality score of 'PET non-viable' segments was higher than that of 'PET viable' segments (1.5 ± 1.0 vs. 0.5 ± 0.7, $P < 0.00001$) (*Figure 3B* right).

Also, the wall motion of the integrated 'PET viable/MRI viable' group was still significantly better than the 'PET non-viable/MRI non-viable' group (0.5 ± 0.7 vs. 1.6 ± 1.0, $P < 0.00001$). Furthermore, still no difference in the wall motion abnormality score was found between the 'PET non-viable/MRI non-viable' segments and the 'PET non-viable/MRI viable' segments (1.6 ± 1.0 vs. 1.1 ± 0.8, $P = $ NS). Interestingly, at follow-up, the wall motion of the 'PET viable/MRI viable' segments was significantly better compared with the 'PET non-viable/MRI viable' segments (0.5 ± 0.7 vs. 1.1 ± 0.8, $P < 0.01$) indicating that the wall motion of these discordant segments tend not to improve as predicted by the impaired FDG uptake (*Figure 3C* right).
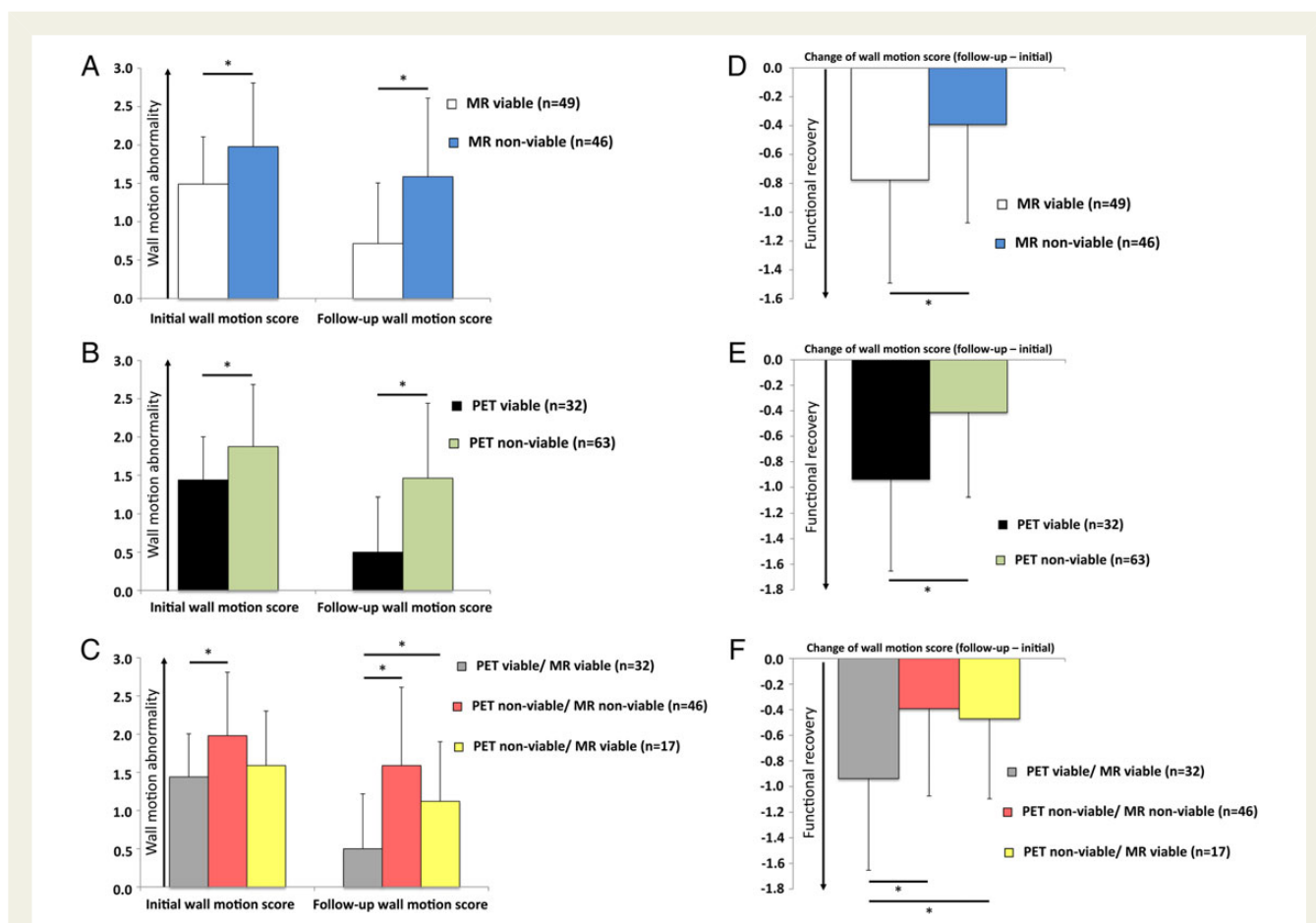

Figure 3 Regional wall motion abnormality and functional recovery in the long-term course. The wall motion abnormality early after AMI and at follow-up as well as the resulting functional recovery of the 95 dysfunctional segments were evaluated regarding different patterns of LGE transmurality and FDG uptake [LGE transmurality (*A* and *D*), FDG uptake (*B* and *E*), combination of LGE transmurality and FDG uptake (*C* and *F*)].

Functional recovery

At follow-up ~6 months after revascularization, 47 of the initially 95 dyskinetic segments (49%) showed a functional improvement. Thirty-two of 'MRI viable' segments (32/49, 65%) and 15 of 'MRI non-viable' segments (15/46, 33%) had a functional recovery of at least one wall motion abnormality point score (*Table 2*). In contrast, 25 'PET viable' segments (25/32, 78%) and 22 'PET non-viable' segments (22/63, 35%) showed a functional improvement (*Table 2*). The functional recovery evaluated by the improvement of wall motion abnormality score was significantly better in the 'MRI viable' group (-0.4 ± 0.7 vs. -0.8 ± 0.7, $P < 0.009$) (*Figure 3D*) and the 'PET viable' group (-0.4 ± 0.7 vs. -0.9 ± 0.7, $P < 0.0007$) (*Figure 3E*).

Twenty-five segments of the 'PET viable/MRI viable' group (25/32, 78%), 15 segments of the 'PET non-viable/MRI non-viable' group (15/46, 33%), and 7 segments of the 'PET non-viable/MRI viable' group (7/17, 41%) showed an improved function (*Table 2*). The decrease of the wall motion abnormality in these three groups was highest in the 'PET viable/MRI viable' group and significantly larger compared with the 'PET non-viable/MRI non-viable' and the 'PET non-viable/MRI viable' group, respectively (-0.9 ± 0.7 vs. -0.4 ± 0.7, $P < 0.002$ and -0.9 ± 0.7 vs. -0.5 ± 0.6, $P < 0.03$), while no difference was observable between 'PET non-viable/MRI non-viable' and 'PET non-viable/MRI viable' segments (-0.4 ± 0.7 vs. -0.5 ± 0.6, $P = $ NS) (*Figure 3F*).

Discussion

To the best of our knowledge, this is the first study that aimed to assess the regional FDG uptake and transmurality of LGE using a fully integrated PET/MRI scanner in the subacute phase after myocardial infarction and compared the recovery of the ischaemically affected myocardium at a 6-month follow-up scan. A regional FDG uptake of >50% compared with remote myocardium is a generally accepted marker for dysfunctional myocardium, which has the potential to improve after revascularization. We aimed to compare the regional FDG uptake with regional LGE transmurality as a marker for functional recovery. LGE transmurality of <50% is another established and generally accepted marker for myocardium tending to recover after revascularization. We found a substantial intermethod agreement for these two parameters in the studied dysfunctional segments, and both parameters were able to differentiate those segments with higher regional wall motion abnormalities. At follow-up, those segments still had a higher mean wall motion abnormality score, and—more important—the change of the wall motion abnormality score as a measure of functional recovery of the segments was significantly higher in the 'MRI viable' or 'PET viable' segments. When the analysis was performed using both LGE transmurality and FDG uptake in an integrated approach, we found that ~18% of the analysed dysfunctional segments showed discrepant results—meaning that these segments were 'PET non-viable' but 'MRI viable'. Our results indicate that these discrepant segments have a wall motion impairment which is comparable to 'PET non-viable/MRI non-viable' segments both early after revascularization as well as at 6-month follow-up and that these segments tend not to improve as good as 'PET viable/MRI viable' segments. In fact, only 41% of these discrepant segments showed an improved wall

motion after 6 months, and the mean score of functional recovery was significantly lower than in 'PET viable/MRI viable' segments.

Our results confirm observations, which were made in prior studies. Kim et al.,[2] performed LGE MRI in patients prior to revascularization therapy and observed the following: 365 of 509 segments (72%) with a LGE transmurality of ≤25% and only 14 of 182 segments (8%) with a LGE transmurality of ≥50% showed an improved wall motion after revascularization. However, 46 of 110 segments (42%) with an LGE transmurality of 26−50% showed an improved wall motion after revascularization, which illustrates the difficulties to predict the outcome of intermediate segments. In a study by Kühl et al.,[28] LGE and FDG PET/^{99m}Tc-sestamibi SPECT were compared regarding the assessment of reversible myocardial dysfunction in chronic heart disease. After coronary artery bypass grafting (CABG) or percutaneous coronary intervention, segments that showed LGE transmurality of ≤50% improved function in 77%, while only 7% of the segments with LGE transmurality >50% and none of the segments with LGE transmurality >75% demonstrated functional recovery. In this study, the pattern of non-transmural LGE but abnormal FDG PET/^{99m}Tc-sestamibi SPECT was also observed, and the authors found an improvement of wall motion in only 42% of the segments. Also, Schvartzman et al.[30] investigated the LGE technique in patients with chronic heart disease and left ventricular function who underwent CABG. In patients who had no evidence of scar, 82% of the segments improved function, whereas only 18% with LGE ≥ 50% recovered.

It needs to be pointed out that the aforementioned studies were performed before revascularization. In this study, however, we measured simultaneously the regional FDG uptake and the transmurality of LGE in a small group of patients early after AMI using a hybrid PET/MRI system. Consequently, these parameters were compared regarding changes of regional wall motion at a MRI follow-up scan after 6 months. In general, studies that aim to predict the improvement of regional wall motion after AMI are rare. Beek et al.[35] imaged 30 patients ~7 days after AMI using a 1.5-T clinical scanner. They found that LGE may be used for the prediction of regional wall motion recovery in patients after AMI and that there is an inverse correlation between the transmurality of LGE and the likelihood of regional function improvement. This finding is in accordance with two further studies: Gerber et al.[36] scanned 25 patients at 4 days after AMI and Choi et al.[37] imaged 24 patients within 7 days of AMI. Also, the number of publications on the utilization of FDG PET for the prediction of LV function outcome in the acute phase of myocardial infarction is low. In a study by Shirasaki et al.,[11] 28 patients were imaged using ^{99m}Tc-tetrofosmin SPECT and FDG PET at ~2 weeks after AMI. Segments that were defined as 'viable' in the acute phase demonstrated a significant improvement of regional wall motion after 6 months while the regional wall motion score showed no difference in segments that were defined as 'non-viable' by FDG PET. So far, to the best of our knowledge only one study exists which solely compares the techniques of LGE or FDG uptake as assessed by simultaneous PET/MRI in patients early after AMI.[38] In this descriptive publication, however, only the feasibility of the technique was tested and modalities were compared. Furthermore, no follow-up assessment was performed in these patients.

Our study has some limitations: first, only a relatively small group of patients who all underwent reperfusion and had mainly small infarcts

was analysed. Consequently, most patients showed a high EF and only minor wall motion abnormalities. Second, for safety reasons patients were imaged when being in a stable health condition, which was at about Day 5–7 after myocardial infarction, and therefore, the regional wall motion might already have been recovered to a certain degree at this time point.

However, our study allows some important conclusions. First of all, we were able to prove that the simultaneous assessment of LGE transmurality and regional FDG uptake—which was standardized in all patients applying the intravenous hyperinsulinaemic-euglycaemic clamp technique—using a hybrid PET/MRI system is feasible. Only one patient had to be removed from the analysis because of poor image quality. Furthermore, we found that both techniques are capable to distinguish those segments, which show a better regional wall motion both post-intervention and at 6-month follow-up. Also, both techniques identified those segments with a significantly better recovery of regional wall motion at follow-up. In the integrated PET/MRI analysis, however, we found a small proportion of segments, which showed discrepant results—meaning that they had a markedly reduced FDG uptake of >50% in comparison to normal myocardium but showed only non-transmural LGE. Only 41% of these segments improved the regional wall motion at follow-up, and furthermore, the functional recovery of these segments was low and comparable to concordant 'PET non-viable/MRI non-viable' segments. This indicates that in these segments, FDG PET is a better predictor for functional recovery regarding a long-term course.

In conclusion, our results suggest that the extent of 'viable' myocardium as assessed by the established thresholds for regional glucose utilization by PET and scar transmurality by MRI are also valid for the prediction of regional wall motion improvement in the subacute phase after myocardial infarction. However, in a small sub-group of segments with discrepant results regarding these parameters, FDG PET might be superior. A possible explanation for this observation might be the fact that the used PET/MRI scanner is equipped with a 3-T MRI component, while the LGE transmurality criteria for the reversibility of wall motion abnormalities were established on a 1.5-Tesla MRI scanner.[2] In general, there is a good agreement in the assessment of LGE between 1.5-T and 3-T MRI;[39] however, significant variation in individual patients has been reported.[40] The main reason for our observation, though, may lie in the fact that the established criteria were—as discussed before—obtained by imaging patients before the elective revascularization in patients suffering from chronic coronary artery disease and not in the subacute phase after revascularization for myocardial infarction.

Last not least, our study indicates that there might be no additional value in the combination of both techniques—LGE MRI and FDG PET—in this specific setting. However, the simultaneous acquisition of PET/MRI for the assessment of FDG uptake and LGE allows to cross-validate both techniques that might also be valuable for future studies.

Acknowledgements

Funding

References

1. Di Carli MF, Davidson M, Little R, Khanna S, Mody FV, Brunken RC *et al.* Value of metabolic imaging with positron emission tomography for evaluating prognosis in patients with coronary artery disease and left ventricular dysfunction. *Am J Cardiol* 1994;**73**:527–33.
2. Kim RJ, Wu E, Rafael A, Chen EL, Parker MA, Simonetti O *et al.* The use of contrast-enhanced magnetic resonance imaging to identify reversible myocardial dysfunction. *New Engl J Med* 2000;**343**:1445–53.
3. Schinkel AF, Poldermans D, Elhendy A, Bax JJ. Assessment of myocardial viability in patients with heart failure. *J Nucl Med* 2007;**48**:1135–46.
4. Camici PG, Prasad SK, Rimoldi OE. Stunning, hibernation, and assessment of myocardial viability. *Circulation* 2008;**117**:103–14.
5. Beanlands RS, Hendry PJ, Masters RG, deKemp RA, Woodend K, Ruddy TD. Delay in revascularization is associated with increased mortality rate in patients with severe left ventricular dysfunction and viable myocardium on fluorine 18-fluoro-deoxyglucose positron emission tomography imaging. *Circulation* 1998;**98**(19 Suppl):II51–6.
6. D'Egidio G, Nichol G, Williams KA, Guo A, Garrard L, deKemp R *et al.* Increasing benefit from revascularization is associated with increasing amounts of myocardial hibernation: a substudy of the PARR-2 trial. *JACC Cardiovascular imaging* 2009;**2**:1060–8.
7. Heyndrickx GR, Millard RW, McRitchie RJ, Maroko PR, Vatner SF. Regional myocardial functional and electrophysiological alterations after brief coronary artery occlusion in conscious dogs. *J Clin Invest* 1975;**56**:978–85.
8. Klein C, Nekolla SG, Balbach T, Schnackenburg B, Nagel E, Fleck E *et al.* The influence of myocardial blood flow and volume of distribution on late Gd-DTPA kinetics in ischemic heart failure. *J Magn Reson Imaging* 2004;**20**:588–93.
9. Klein C, Schmal TR, Nekolla SG, Schnackenburg B, Fleck E, Nagel E. Mechanism of late gadolinium enhancement in patients with acute myocardial infarction. *J Cardiovasc Magn Reson* 2007;**9**:653–8.
10. Kwong RY, Chan AK, Brown KA, Chan CW, Reynolds HG, Tsang S *et al.* Impact of unrecognized myocardial scar detected by cardiac magnetic resonance imaging on event-free survival in patients presenting with signs or symptoms of coronary artery disease. *Circulation* 2006;**113**:2733–43.
11. Shirasaki H, Nakano A, Uzui H, Yonekura Y, Okazawa H, Ueda T *et al.* Comparative assessment of 18F-fluorodeoxyglucose PET and 99mTc-tetrofosmin SPECT for the prediction of functional recovery in patients with reperfused acute myocardial infarction. *Eur J Nucl Med Mol Imaging* 2006;**33**:879–86.
12. National Diabetes Data Group. Classification and diagnosis of diabetes mellitus and other categories of glucose intolerance. *Diabetes* 1979;**28**:1039–57.
13. Summary of the second report of the National Cholesterol Education Program (NCEP) Expert Panel on Detection, Evaluation, and Treatment of High Blood Cholesterol in Adults (Adult Treatment Panel II). *J Am Med Assoc* 1993;**269**:3015–23.
14. National Cholesterol Education Program Expert Panel on Detection, Evaluation, and Treatment of High Blood Cholesterol in Adults. Third Report of the National Cholesterol Education Program (NCEP) Expert Panel on Detection, Evaluation, and Treatment of High Blood Cholesterol in Adults (Adult Treatment Panel III) final report. *Circulation* 2002;**106**:3143–421.
15. Whelton PK. Epidemiology of hypertension. *Lancet* 1994;**344**:101–6.
16. Torigian DA, Zaidi H, Kwee TC, Saboury B, Udupa JK, Cho ZH *et al.* PET/MR imaging: technical aspects and potential clinical applications. *Radiology* 2013;**267**:26–44.
17. Delso G, Furst S, Jakoby B, Ladebeck R, Ganter C, Nekolla SG *et al.* Performance measurements of the Siemens mMR integrated whole-body PET/MR Scanner. *J Nucl Med* 2011;**52**:1914–22.
18. Drzezga A, Souvatzoglou M, Eiber M, Beer AJ, Furst S, Martinez-Moller A *et al.* First clinical experience with integrated whole-body PET/MR: comparison to PET/CT in patients with oncologic diagnoses. *J Nucl Med* 2012;**53**:845–55.

19. Souvatzoglou M, Fuerst S, Foerster S, Eiber M, Nekolla S, Ziegler S et al. Comparison of simultaneous [18F]FET PET/MR with PET/CT in patients with cerebral tumours. *Eur J Nucl Med Mol Imaging* 2012;**39**:S245–6.

20. Souvatzoglou M, Eiber M, Takai T, Fuerst S, Drzezga A, Ziegler S et al. Intergrated simultaneous [C-11]choline PET/MR in patients with prostate cancer. Comparison with PET/CT. *Eur J Nucl Med Mol Imaging* 2012;**39**:S254–5.

21. Eiber M, Souvatzoglou M, Geinitz H, Rummeny EJ, Schwaiger M, Beer AJ. First clinical experience in restaging of patients with recurrent prostate cancer by 11C-Choline-PET/MR: comparison with 11C-Choline-PET/CT. *Eur J Nucl Med Mol Imaging* 2012;**39**(Suppl 2):S174.

22. Boehm J, Haas F, Bauernschmitt R, Wagenpfeil S, Voss B, Schwaiger M et al. Impact of preoperative positron emission tomography in patients with severely impaired LV-function undergoing surgical revascularization. *Int J Cardiovasc Imaging* 2010;**26**: 423–32.

23. DeFronzo RA, Tobin JD, Andres R. Glucose clamp technique: a method for quantifying insulin secretion and resistance. *Am J Physiol* 1979;**237**:E214–23.

24. Martinez-Moller A, Souvatzoglou M, Delso G, Bundschuh RA, Chefd'hotel C, Ziegler SI et al. Tissue classification as a potential approach for attenuation correction in whole-body PET/MRI: evaluation with PET/CT data. *J Nucl Med* 2009;**50**: 520–6.

25. Nuyts J, Bal G, Kehren F, Fenchel M, Michel C, Watson C. Completion of a truncated attenuation image from the attenuated PET emission data. *IEEE Trans Med Imaging* 2013;**32**:237–46.

26. Huber AM, Schoenberg SO, Hayes C, Spannagl B, Engelmann MG, Franz WM et al. Phase-sensitive inversion-recovery MR imaging in the detection of myocardial infarction. *Radiology* 2005;**237**:854–60.

27. Cerqueira MD, Weissman NJ, Dilsizian V, Jacobs AK, Kaul S, Laskey WK et al. Standardized myocardial segmentation and nomenclature for tomographic imaging of the heart. A statement for healthcare professionals from the Cardiac Imaging Committee of the Council on Clinical Cardiology of the American Heart Association. *Circulation* 2002;**105**:539–42.

28. Kuhl HP, Lipke CS, Krombach GA, Katoh M, Battenberg TF, Nowak B et al. Assessment of reversible myocardial dysfunction in chronic ischaemic heart disease: comparison of contrast-enhanced cardiovascular magnetic resonance and a combined positron emission tomography-single photon emission computed tomography imaging protocol. *Eur Heart J* 2006;**27**:846–53.

29. Bove CM, DiMaria JM, Voros S, Conaway MR, Kramer CM. Dobutamine response and myocardial infarct transmurality: functional improvement after coronary artery bypass grafting--initial experience. *Radiology* 2006;**240**:835–41.

30. Schvartzman PR, Srichai MB, Grimm RA, Obuchowski NA, Hammer DF, McCarthy PM et al. Nonstress delayed-enhancement magnetic resonance imaging of the myocardium predicts improvement of function after revascularization for chronic ischemic heart disease with left ventricular dysfunction. *Am Heart J* 2003; **146**:535–41.

31. Ibrahim T, Hackl T, Nekolla SG, Breuer M, Feldmair M, Schomig A et al. Acute myocardial infarction: serial cardiac MR imaging shows a decrease in delayed enhancement of the myocardium during the 1st week after reperfusion. *Radiology* 2010; **254**:88–97.

32. Nekolla SG, Miethaner C, Nguyen N, Ziegler SI, Schwaiger M. Reproducibility of polar map generation and assessment of defect severity and extent assessment in myocardial perfusion imaging using positron emission tomography. *Eur J Nucl Med* 1998;**25**:1313–21.

33. Castellani M, Colombo A, Giordano R, Pusineri E, Canzi C, Longari V et al. The role of PET with 13N-ammonia and 18F-FDG in the assessment of myocardial perfusion and metabolism in patients with recent AMI and intracoronary stem cell injection. *J Nucl Med* 2010;**51**:1908–16.

34. Baer FM, Voth E, Deutsch HJ, Schneider CA, Horst M, de Vivie ER et al. Predictive value of low dose dobutamine transesophageal echocardiography and fluorine-18 fluorodeoxyglucose positron emission tomography for recovery of regional left ventricular function after successful revascularization. *J Am Coll Cardiol* 1996;**28**:60–9.

35. Beek AM, Kuhl HP, Bondarenko O, Twisk JW, Hofman MB, van Dockum WG et al. Delayed contrast-enhanced magnetic resonance imaging for the prediction of regional functional improvement after acute myocardial infarction. *J Am Coll Cardiol* 2003;**42**:895–901.

36. Gerber BL, Garot J, Bluemke DA, Wu KC, Lima JA. Accuracy of contrast-enhanced magnetic resonance imaging in predicting improvement of regional myocardial function in patients after acute myocardial infarction. *Circulation* 2002;**106**:1083–9.

37. Choi KM, Kim RJ, Gubernikoff G, Vargas JD, Parker M, Judd RM. Transmural extent of acute myocardial infarction predicts long-term improvement in contractile function. *Circulation* 2001;**104**:1101–7.

38. Nensa F, Poeppel TD, Beiderwellen K, Schelhorn J, Mahabadi AA, Erbel R et al. Hybrid PET/MR imaging of the heart: feasibility and initial results. *Radiology* 2013; **268**:366–73.

39. Oshinski JN, Delfino JG, Sharma P, Gharib AM, Pettigrew RI. Cardiovascular magnetic resonance at 3.0 T: current state of the art. *J Cardiovasc Magn Reson* 2010;**12**:55.

40. Huber A, Bauner K, Wintersperger BJ, Reeder SB, Stadie F, Mueller E et al. Phase-sensitive inversion recovery (PSIR) single-shot TrueFISP for assessment of myocardial infarction at 3 tesla. *Invest Radiol* 2006;**41**:148–53.